# THE TIME DEPENDENT MAGNETOHYDRODYNAMIC GENERATOR

by

David A. Oliver

GTL Report No. 115 March 1974

GAS TURBINE LABORATORY
MASSACHUSETTS INSTITUTE OF TECHNOLOGY
CAMBRIDGE, MASSACHUSETTS

# THE TIME DEPENDENT MAGNETOHYDRODYNAMIC GENERATOR

by

David A. Oliver

GTL Report No. 115 March 1974

## ACKNOWLEDGEMENTS

This work was supported by the National Science Foundation under Grant GK-38130 and by the Office of Coal Research, U.S. Department of the Interior.

The author would like to acknowledge the assistance of Messrs. Stephen Jardin and Steven Seffens with the calculations presented in this paper.

TABLE OF CONTENTS

# THE TIME DEPENDENT MAGNETOHYDRODYNAMIC GENERATOR

## I. Introduction

Low magnetic Reynolds number magnetohydrodynamic generators as would be utilized in power plants are conceived of as steady state D.C. devices. Unsteady phenomena may exist in such generators however. Fluctuations induced fluid mechanically or through combustion may develop into amplifying magnetoacoustic instabilities[1,2,3]. In addition to possible instabilities appearing in the bulk of the flow, there exist other important unsteady situations in which the generator must operate. These include the transient response of the generator to changes in load conditions, start up and shut down, coupled unsteady interactions of the generator with the power grid, and the response of the generator to faults such as electrode wall break down or the sudden imposition of a short along the insulator wall. Many of these unsteady situations involve large changes in the amplitudes of the fluid mechanical and electrical variables and therefore require a large amplitude unsteady theory.

In the present work we present a description of unsteady quasi one dimensional magnetohydrodynamic generator flows and propose a highly accurate explicit time dependent method of predicting the time response of such flows. This method of calculation is capable of treating MHD flows under subsonic, supersonic, and transonic flow conditions, arbitrary nonuniformities in electric fields and currents, strong interaction parameters, and with normal shocks present in the duct.

In Part II a formulation of the appropriate magnetohydrodynamic fluid equations for quasi-one-dimensional flow is given. In Part III a description of the Lorentz forces and Lorentz power in the flow is given.

In Part IV a finite difference operator for the unsteady nonlinear MHD equations is proposed and its stability and accuracy characteristics are described. In Parts VI and VII, illustrations of this analysis are presented for two unsteady generator situations of contemporary interest: (1) the growth and evolution of large amplitude magnetoacoustic fluctuations under conditions of strong interaction, and (2) the behavior of the generator to changes in loading.

## II. Unsteady Fluid Conservation Equations

In the quasi-one-dimensional approximation transverse variations are neglected compared to axial variations in a single flow direction. The fluid may be described in terms of its velocity distribution u and two thermodynamic variables such as its density $\rho$ and internal energy $\varepsilon$. In addition, the flow cross sectional area A becomes a variable describing the flow. It will be assumed that the area A is invariant in time and is specified as a given function of the axial coordinate of the flow. In terms of the mass density $\rho$, momentum density m where $m = \rho u$, and the total energy density $e = \varepsilon + u^2/2$ the fluid state may be represented at any time t and spatial location x along the axis of the flow by the vector function $\underline{U}(x,t)$:

$$\underline{U}(x,t) = \begin{pmatrix} \rho \\ m \\ e \end{pmatrix} \tag{1}$$

The fluid state $\underline{U}$ is governed by the quasi one-dimensional fluid conservation equations which in the magnetohydrodynamic regime assume the form

$$(\underline{U})_t = -(\underline{F})_x - \underline{H} - \underline{D} + \underline{S} \tag{2}$$

The vector $\underline{F}$ describes the mass, momentum, and energy fluxes of the

fluid:

$$\underline{F}(\underline{U}) = \begin{pmatrix} m \\ m^2/\rho + p \\ (e+p)\ m/\rho \end{pmatrix} \tag{3}$$

The vector $\underline{H}$ describes the area variation effect:

$$\underline{H}(\underline{U},x) = A^{-1}(A)_x \begin{pmatrix} m \\ m^2/\rho \\ (e+p)\ m/\rho \end{pmatrix} \tag{4}$$

The vector $\underline{S}$ contains the Lorentz force and power. If the electrical state is described in terms of a current density $\vec{J}$, electrical field $\vec{E}$, and magnetic field $\vec{B}$, then

$$\underline{S}(\underline{U},x,t) = \begin{pmatrix} 0 \\ \vec{J}\times\vec{B}_x \\ \vec{J}\cdot\vec{E} \end{pmatrix} \tag{5}$$

For a flow in which the velocity $\vec{u}$ is normal to $\vec{B}$ and $\vec{E}$, $\vec{J}$ exist in the plane normal to $\vec{B}$ with components $E_x$, $E_y$, $J_x$, $J_y$ the Lorentz force and power are

$$\vec{J}\times\vec{B}_x = J_y B$$

$$\vec{J}\cdot\vec{E} = J_x E_x + J_y E_y$$

The vector $\underline{D}$ contains the effects of wall friction and heat transfer:

$$\underline{D}(\underline{U},x,t) = \begin{pmatrix} 0 \\ 4\tau_w/D_H \\ 4q_w/D_H \end{pmatrix} \tag{6}$$

where $\tau_w$ and $q_w$ are the wall shear stress and heat flux respectively. The

wall shear stress and heat flux may be described by the appropriate wall region boundary layer mechanics which relate these quantities to the mean flow variables $\rho$, u, e and the wall boundary conditions. These relationships are summarized by the statements

$$\tau_w = N_f \frac{\rho u^2}{2} = N_f \frac{m^2}{2\rho} \tag{7}$$

$$q_w = N_{st}\rho u c_p (T_w - T_{aw}) + q_r \tag{8}$$

where $N_f$ and $N_{st}$ are the friction factor and Stanton numbers respectively. The adiabatic wall temperature is $T_{aw}$ and $T_w$ is the wall temperature. The radiative contribution to the wall heat flux is $q_r$. The friction factor and Stanton numbers are functions of the Reynolds number $N_R$ and Mach number M:

$$\begin{aligned} N_f &= N_f(N_R, M) \\ N_{st} &= N_{st}(N_R, M) \end{aligned} \tag{9}$$

The fluid equations are completed by equations of state of the form

$$\begin{aligned} p &= p(\rho, \varepsilon) \\ T &= T(\rho, \varepsilon) \end{aligned} \tag{10}$$

where $\varepsilon$ is given in terms of $\rho$, m, e by

$$\varepsilon = (e - m^2/2\rho)/\rho$$

## III. Electrical Description

In the low magnetic Reynolds number approximation the magnetic field $\vec{B}$ is imposed and is uninfluenced by the currents flowing in the gas. This field is then given as a function of x,t as $\vec{B}(x,t)$. The local electric fields and currents $J_x$, $J_y$, $E_x$, $E_y$ which exist depend upon the generator loading, external connection, and the local fluid state $\underline{U}$ since the currents depend upon the local velocity $u = m/\rho$ and the electrical conductivity

depends upon the local fluid thermodynamic state. One independent pair of the four electric fields and currents [such as $(E_x,E_y)$, $(J_x,J_y)$, $(E_x,J_y)$, $(E_y,J_x)$] must be specified to determine the electrical state at each location in the duct. The remaining variables are then determined by the conditions of Ohm's law:

$$\begin{aligned} J_x + \beta J_y &= \sigma E_x \\ -\beta J_x + J_y &= \sigma(\bar{E}_y - uB - \Delta V/h) \end{aligned} \tag{11}$$

If voltage drops of total magnitude $\Delta V$ are present at the electrodes, the average electric field $\bar{E}_y$ over the electrode separation h is related to the electric field in the core of the flow $E_y$ as

$$\bar{E}_y = E_y + \Delta V/h$$

The electrical conductivity $\sigma$ and the Hall parameter $\beta$ are functions of the local thermodynamic state of the gas:

$$\sigma = \sigma(\rho,T)$$

$$\beta = \beta(\rho,T)$$

The external connection of the generator can be specified in terms of axial and transverse loading parameters $K_x$, $K_y$ defined by

$$\begin{aligned} E_x &= -K_x/\beta uB \\ \bar{E}_y &= K_y uB \end{aligned} \tag{12}$$

The transverse load conductance (reciprocal impedance) may also be used to specify the local fields in lieu of $\bar{E}_y$. For the Faraday generator in which $J_x = 0$ and $K_x = 1 - K_y$ the load conductance per unit channel length $\sigma_L$ is related to $K_y$ as

$$K_y = (1 + \sigma_L/\sigma)^{-1} \tag{13}$$

The transverse load impedance R for a channel segment of length $\delta x$,

depth d, and height h is given in terms of the load conductance $\sigma_L$ by

$$R = (\sigma_L \frac{d}{h} \delta x)^{-1} \tag{14}$$

In a single load diagonal generator conservation of current requires that

$$J_x - \tan\theta\, J_y = I/A(x) \tag{15}$$

where I is the generator load current, A(x) is the local cross sectional area of the duct, and $\theta$ is the angle of the equipotentials relative to the normal to the channel axis:

$$\overline{E}_y - \tan\theta\, E_x = 0 \tag{16}$$

For the Faraday generator the specification of $K_y$ (or $\sigma_L$) and $K_x$ is usual. For the single load diagonal connection specification of I and $\theta$ is usual. Note that the limit $\theta = 0$ of the single load diagonal connection is the Hall generator connection. For the Faraday generator the load voltage $V_y(x,t)$ is given by

$$V_y(x,t) = -\overline{E}_y(x,t)h(x) \tag{17}$$

where h(x) is the local channel height. The load conductances $\sigma_L(x,t)$ are related to the local currents and fields as

$$\sigma_L(x,t) = -\frac{J_y(x,t)}{\overline{E}_y(x,t)} \tag{18}$$

For the single load diagonal connection the load voltage is given by

$$V_x(t) = -\int_0^L E_x(x,t)dx \tag{19}$$

The load impedance for such a generator $R_L(t)$ is then related to the load current I(t) and the load voltage $V_x(t)$ as

$$R_L(t) = \frac{V_x(t)}{I(t)} \tag{20}$$

Using the Ohm's law (11) and the channel connection conditions (15) and (16) the axial electric field may be expressed in terms of I and θ as

$$E_x = -\frac{\beta+\tan\theta}{1+\tan^2\theta}(1-\overline{\Delta V})uB + \frac{1+\beta^2}{1+\tan^2\theta}\left(\frac{L}{\sigma A}\right)\frac{I}{L}$$

The voltage between the ends of the generator may then be expressed as

$$V_x = V_{xo} - IR_i \tag{21}$$

where $R_i$ is the internal impedance of the generator:

$$R_i = \left\langle \frac{1+\beta^2}{1+\tan^2\theta}\left(\frac{L}{\sigma A}\right)\right\rangle \tag{22}$$

and $V_{xo}$ is the open circuit voltage:

$$V_{xo} = \left\langle \frac{\beta+\tan\theta}{1+\tan^2\theta}(1-\overline{\Delta V})uB\right\rangle L \tag{23}$$

The average < > is over the channel length L. The load current is then

$$I = \frac{V_{xo}}{R_i+R_L} \tag{24}$$

and the short circuit current is

$$I_s = \frac{V_{xo}}{R_i} \tag{25}$$

## IV. Boundary and Initial Conditions

An unsteady magnetohydrodynamic channel flow involves the specification of an initial fluid state $\underline{U}(x,0)$ from which the subsequent fluid states are computed for given electrical loading specification and boundary condition variation. The boundary conditions require the specification of the fluid states $\underline{U}(0,t)$, $\underline{U}(L,t)$.

The initial condition is the specification of the fluid state $\underline{U}^o(x)$ at all points in the flow at time t = 0:

$$\underline{U}(x,0) = \underline{U}^{o}(x) \tag{26}$$

The boundary conditions are specifications of the fluid state as functions of time at the channel boundaries x = 0, x = L:

$$\begin{aligned} \underline{U}(0,t) &= \underline{U}_{o}(t) \\ \underline{U}(L,t) &= \underline{U}_{L}(t) \end{aligned} \tag{27}$$

The initial value problem is then completely specified in terms of the initial function $\underline{U}^{o}(x)$ and the boundary functions $\underline{U}_{o}(t)$, $\underline{U}_{L}(t)$. In addition, the electrical boundary conditions must be specified as functions of time. For the Faraday generator this condition may be the specification of the load conductance function $\sigma_{L}(x,t)$. For the single load diagonal generator, this specification may be the load impedance $R_{L}(t)$.

At each time step the electric field and current distributions are computed corresponding to the fluid state existing at that instant and the electrical boundary conditions imposed. For example, in the Faraday generator case if the load conductance is specified as a function of time as $\sigma_{L}(x,t)$ the loading parameter distributions are determined as

$$K_{y}(x,t) = \frac{1}{1+\sigma_{L}(x,t)/\sigma(x,t)}$$

$$K_{x}(x,t) = 1 - K_{y}(x,t)$$

The complete electrical distribution is then determined by $K_{y}(x,t)$, $K_{x}(x,t)$. In the case of a single load diagonal generator, if the load impedance $R_{L}(t)$ is specified as a function of time and the diagonal connection angle $\theta(x)$ is specified and independent of time, the load current I(t) is given at each instant by

$$I(t) = \frac{V_{xo}(t)}{R_{i}(t)+R_{L}(t)}$$

where $V_{xo}$ is given by Eq. (23) and $R_i$ is given by Eq. (22).

## V. Method of Solution

We now propose a method for solving the first order vector differential Eq. (2) for the fluid state $\underline{U}(x,t)$. The governing equation may be expressed as

$$(\underline{U})_t = -[\underline{F}(\underline{U})]_x + \underline{C}(\underline{U},x,t) \tag{28}$$

where the undifferentiated terms are

$$\underline{C}(\underline{U},x,t) = -\underline{H}(\underline{U},x) + \underline{S}(\underline{U},x,t) - \underline{D}(\underline{U},x,t) \tag{29}$$

Our approach will be based upon replacing the nonlinear partial differential operator in Eq. (28) by a nonlinear finite difference operator. For this purpose we consider the space and time coordinates to be discretized with finite differences $\delta x$, $\delta t$ such that

$$x = j\delta x$$

$$t = n\delta t$$

where j and n are integers. The state $\underline{U}$ at time t and location x is then represented as $\underline{U}(x,t) = \underline{U}_j^n$. The finite difference form of Eq. (28) is then

$$\underline{U}_j^{n+1} = L\underline{U}_j^n \tag{30}$$

where $L$ is an appropriate finite difference operator for Eq. (28). An operator $L$ with attractive accuracy and computational economy is the two step operator in which $L$ is formed by first calculating an intermediate state $\underline{U}_j^*$ as

$$\underline{U}_j^* = \underline{U}_j^n - \frac{\delta t}{\delta x}[\underline{F}(\underline{U}_{j+1}^n) - \underline{F}(\underline{U}_j^n)] + \delta t\underline{C}(\underline{U}_j^n,x,t) \tag{31a}$$

The final fluid state is then determined as

$$\underline{U}_j^{n+1} = 1/2\ \{\underline{U}_j^n + \underline{U}_j^* - \frac{\delta t}{\delta x}[\underline{F}(\underline{U}_j^*) - \underline{F}(\underline{U}_{j-1}^*)] + \delta t\underline{C}(\underline{U}_j^*,x,t)\} \tag{31b}$$

Thus, given the initial fluid state $\underline{U}_j^o$ the subsequent fluid states may be computed forward in time. The finite difference operator (31) is a modification of a class of second order accurate operators developed by Lax and Wendroff,[4] Richtmyer,[5] and MacCormack.[6] They have the power to compute flows in the full subsonic, transonic, and supersonic range including moving internal shockwaves, rarefaction waves, and contact discontinuities. These discontinuities are represented as rapidly varying regions in the mesh which are spread over three to four mesh points. The operator is second order in the sense that the finite difference operator deviates from the partial differential operator in terms that are of order $\delta t^2$, $\delta x^2$, $\delta t \delta x$ in the finite difference increments. Operators which are only first order accurate do not resolve the flow structure as sharply as the second order accurate operators. Operators of higher order accuracy require larger amounts of computing time per mesh point. The second order accurate operator is a good compromise between accuracy and computational economy.

The numerical stability of the operator (31) is conditional and requires that the Courant condition[7] be satisfied at each point in the flow:

$$\delta t \leq \frac{\delta x}{|u|+c}$$

The time step $\delta t$ is thus limited for a given space step $\delta x$ by the fluid speed $|u|$ and the sonic speed c.

The undifferentiated term $\underline{C}(\underline{U},x,t)$ does not affect the numerical stability conditions; however, for accuracy of the computed results the time step $\delta t$ should satisfy the condition

$$\delta t \ll (\lambda_c)_{max}^{-1}$$

where the $\lambda_c$ are the eigenvalues of the Jacobian matrix $\partial \underline{C}/\partial \underline{U}$. These eigenvalues are the growth or decay rates of the linearized system

$$(\underline{U})_t = \frac{\partial \underline{C}}{\partial \underline{U}} \underline{U}$$

This requirement in physical terms is that the time step $\delta t$ should be small enough so that the fluid state changes by only a small fraction over the time $\delta t$ under the action of area variation, Lorentz forces, wall heat conduction, and wall shear stress.

## VI. Load Change Transients

As a first illustration of the foregoing unsteady theory of the MHD generator we shall consider a description of a strong generator transient initiated by a load change. A constant velocity supersonic single load diagonal wall generator is operating at the steady state conditions given in Table VI-1. At time $t = 0$, the load is instantly shorted and remains

Table VI-1 Steady State Operating Conditions of Constant Velocity Single Load Diagonal Wall MHD Generator

| | |
|---|---|
| Velocity | 1500 m/sec |
| Magnetic Field Strength | 4 Tesla |
| Length | 4.5 m |
| Mass Flow | 250 kg/sec |
| Wall Angle | 45° |
| Operating Voltage | 7554 volts |
| Operating Current | 6358 amps |
| Inlet Temperature | 2260° K |
| Inlet Pressure | 2 atm |
| Exit Temperature | 2107° K |
| Exit Pressure | 1.2 atm |

shorted [$R_L(t) = 0$, $t \geq 0$]. The response of the generator to this load

change is then determined. The working fluid is assumed to be an ideal gas with specific heat ratio $\gamma = 1.2$ and molecular weight MW = 30. The thermodynamic and electrical transport properties are represented in terms of the functions described in Appendix II. Wall friction and heat transfer are neglected in this illustration ($\underline{D} \equiv 0$).

The response of the pressure in the generator is shown in Fig. 1. The flow time through the generator at the initial steady state velocity (1500 m/sec) is 3 ms. By t = 3 ms the pressure has begun to rise sharply in the upstream region of the generator due to the increased deceleration of the gas induced by the short circuit Lorentz forces. By t = 4 ms the flow has been decelerated below Mach 1. The sonic point is first reached at the exit of the generator ahead of the diffuser at t = 2.9 ms. Further deceleration continues in the downstream generator region which leads to the formation of a shock wave which is quite well developed by t = 5 ms. The shock wave strengthens and moves upstream slowly. Behind the shock the temperature of the constant property gas has risen sharply so that the electrical conductivity behind the shock is nearly an order of magnitude greater than the conductivity ahead of the shock. By t = 6 ms the shock is still moving upstream and will eventually reach the generator inlet.

The response of the load current and pressure at the center of the channel are shown in Fig. 2. Initially the current rises to reach a peak short circuit current value of nearly 90,000 amperes at t = 4 ms. By this time, however, the shock has formed and begun moving upstream and the flow is increasingly decelerated so that the current begins to fall as rapidly as it rose. The fluctuation in the channel center pressure is also related to the formation and passage of the shock wave and the continued deceleration of the flow.

In Fig. 3, the detailed pressure distribution and current distribution throughout the generator are shown at t = 6.4 ms. Because the wall angle is fixed during the transient, the axial current $J_x$ has grown to be nearly the same order of magnitude as the transverse current $J_y$ during the deceleration of the flow. The detailed distribution of current and pressure in the vicinity of the shock wave are shown in Fig. 4. The method of computation represents the shock as a rapidly varying region over about 3-6 mesh points. The fluid state inside this region is not the actual fluid state within such a shock wave; however, because of the conservation law differencing of the fluid equations, the conditions on either side of the shock are quite accurately computed.

As a second illustration, we consider a load change transient initiated by a change in seed level of the generator while all other boundary conditions including the load resistances remain fixed. The generator to be subjected to this transient is a multiple load diagonal wall generator, whose steady state operating conditions are given in Table VI-2.

Table VI-2 Design Characteristics of Steady State Multiple Load Diagonal Wall Generator, Constant Velocity, Constant Electrical Efficiency, $J_x = 0$.

| | |
|---|---|
| Velocity | 750 m/sec |
| Inlet Temperature | 2550° K |
| Inlet Pressure | 4 atm |
| Magnetic Field | 6 Tesla |
| Length | 12 meters |
| Exit Temperature | 2190° K |
| Exit Pressure | 1.18 atm |
| Electrical Efficiency | 0.75 |

At time t = 2ms, the seed level to this generator is instantly reduced by

a factor of 4 and the response of the generator is computed. The space-time history of the important fluid and electrical variables is shown in Fig. 5. It can be seen that as the seed reduction wave passes through the generator, the current levels fall and the reduced Lorentz forces allow the flow to accelerate. Since the conductivity is nearly proportional to the square root of the seed density for weak ionization, it can be seen that a factor of four reduction in seed density has reduced the transverse currents in the generator by approximately a factor of two. Because the diagonal wall angle remains fixed during this transient, the angle is off design for the new current level and thus a significant axial current $J_x$ now flows over most of the generator in the final steady state.

## VII. Nonlinear Stability of MHD Generators

As a second illustration of the time-dependent MHD generator theory, we consider the stability of MHD generator flows to small disturbances in the inlet state.*

The particular disturbance to be studied is the archetypal one of the propagation of a disturbance through the generator initiated by the imposition of a pressure pulse at the inlet of the generator. If a disturbance is initiated at the inlet of a supersonic generator flow in the absence of Lorentz forces and in the absence of steady state gradients the disturbance will propagate as three distinct modes traveling at the three speeds u + c (downstream mode), u (entropy mode), and u - c (upstream mode) where u and c are the fluid and sonic speeds respectively. With

---

*This work is described more fully in D. A. Oliver, "Nonlinear Stability of Magnetohydrodynamic Generators" submitted to the 1974 AIAA Fluid and Plasmadynamics Conference.

steady state gradients and Lorentz forces present these propagation speeds will be altered for different wavelength disturbances since the system is then dispersive; however, for disturbances with wavelengths which are not too long relative to the channel length these propagation speeds are not very different from their free space values.

In the transient we shall now describe the steady generator flow was subjected to a square wave pressure pulse at the generator inlet. The static pressure at the inlet was increased over the steady inlet pressure $p_i$ by the fractional amount $\Delta p/p_i$ for the time duration $\tau$. The steady state generator flow described in Table VII-1 was used as the basis

Table VII-1 Conditions for Steady State Diagonal Wall MHD Generator

| | |
|---|---|
| Velocity | 1500 m/sec |
| Magnetic Field | 4 Tesla |
| Wall Angle | 45° |
| Inlet Temperature | 2500° K |
| Inlet Pressure | 2 atm |
| Inlet Current | |
| $J_x$ | 0.67 amp/cm$^2$ |
| $J_y$ | 1.07 amp/cm$^2$ |

of these studies. This is a single load diagonal wall generator with fixed wall angle. The load impedance during the disturbance transients to be described was held fixed and the generator current and voltage evolved so as to match this fixed load impedance; hence full coupling of the generator through the load circuit is included in these calculations.

Linearized stability theory (assuming wavelengths short compared to the channel length) may be applied to MHD channel flows with Lorentz forces and gradients. [8, 9] For the steady state design described in

Table VII-1, the linear stability theory predicts that the upstream and downstream modes [10] are slightly damped; however, the entropy mode will grow.[11] This generator is therefore linearly unstable to the entropy mode; however, this instability is a convective instability and small disturbances may propagate out of the generator before growing to a size which would be significant compared to the steady flow.

We shall now examine the stability characteristics of such an MHD generator described by the full fluid equations without linearizing approximations using the unsteady theory and technique of the present work. A disturbance of $\Delta p/p_i = 0.06$ for a duration $\tau = 0.08$ ms was initiated at the inlet of the generator described in Table VII-1. The response of this convectively unstable generator to this disturbance is shown in Fig. 6. The entropy wave of the perturbation has grown to 30% of the amplitude of the steady flow by t = 1 ms; a factor of 5 increase over its initial amplitude. By the time the entropy wave of the disturbance has been convected through slightly more than half the channel, it has grown to be of the order of the steady state pressure. At this time the steady flow is so strongly disturbed that a normal shock wave forms, followed by a rapid acceleration of the flow downstream of the shock. The convective instability thus leads to global instability of the generator. The propagating entropy pulse (and the Lorentz force disturbance propagating with it) acts like a throat which shocks the flow at the upstream side of the pulse and re-expands the flow on the downstream side (the Lorentz force at the upstream side is greater than the mean Lorentz force while that on the downstream side is much less than the mean which allows the flow to accelerate).

The transformation of the convective instability to a global instability arises from the fact that finite amplitude disturbances grow faster than infinitesimal disturbances as discussed in Ref. 11. For initial disturbances less than $\Delta p/p_i = 0.3\%$, the computed nonlinear distributions are within 1% of the predictions of linear theory. For disturbances of only 2%, however, significant deviation from the linear theory results. Waves corresponding to an initial disturbance of 2.5% grow to 5 times the linear prediction in a single transient through the generator.

Fluctuations in the fluid state exert a major influence on the Lorentz force and power through the electrical conductivity. For weak ionization of a singly ionized substance whose ionization potential is $\varepsilon_i$ the fluctuation in conductivity $\sigma$ is related to the fluctuation in temperature approximately as

$$\frac{\Delta\sigma}{\sigma_i} = \left(\frac{\varepsilon_i}{2kT_i}\right) \frac{\Delta T}{T_i}$$

Since the factor $\varepsilon_i/2kT_i$ is of the order of 10 for the steady state generator of interest, a 2% temperature fluctuation corresponds to a conductivity fluctuation in excess of 20%. It is the sensitivity of the conductivity to the fluid temperature which makes the onset of nonlinear effects in MHD generator stability occur for such small amplitude of the fluid disturbances.

## VIII. Conclusion

A nonlinear unsteady theory for magnetohydrodynamic flows capable of treating such flows under subsonic, supersonic, and transonic flow conditions, axial nonuniformities in fields and currents, and strong interaction parameters has been proposed. The theory is implemented with an explicit finite-difference procedure of high order accuracy. This theory, illustrated

for load change transients and inlet state perturbations, may be utilized for the prediction of general transient behavior of a wide variety for MHD generators of contemporary and future interest.

## APPENDIX I. VARIABLE SEEDING

In some situations, the seed injection to the generator is controlled as a function of time so that the seed function is not a constant throughout the generator. In such conditions the unionized seed mass density $\rho_{so}$ is introduced as an additional state variable. The fluid state vector then becomes

$$\underline{U} = \begin{Bmatrix} \rho \\ \rho_{so} \\ m \\ e \end{Bmatrix}$$

The interaction bectors then simply become 4 vectors as

$$\underline{F} = \begin{Bmatrix} m \\ \frac{\rho_{so}}{\rho} m \\ m^2/\rho + p \\ (e+p)\ m/\rho \end{Bmatrix}$$

$$\underline{H} = A^{-1}A_x \begin{Bmatrix} m \\ (\frac{\rho_{so}}{\rho})m \\ m^2/\rho \\ (e+p)\ m/\rho \end{Bmatrix}$$

$$\underline{S} = \begin{Bmatrix} 0 \\ 0 \\ (J\times B)_x \\ J\cdot E \end{Bmatrix}$$

$$\underline{D} = \begin{Bmatrix} 0 \\ 0 \\ 4\tau_w/D_H \\ 4q_w/D_H \end{Bmatrix}$$

The electrical conductivity is then a function of the local $\rho$, $\rho_{so}$, T:

$$\sigma = \sigma(\rho,\rho_{so},T)$$

$$\beta = \beta(\rho,\rho_{so},T)$$

Boundary and initial conditions are now required for $\rho_{so}$. A typical transient may invoke the specification of an initial steady state in which $\rho_{so}(x)$ is specified as a fixed fraction of the gas density $\rho(x)$ throughout the channel. The inlet boundary condition may then be the function $\rho_{so}(0,t)$ which is prescribed according to the seed control transient of interest. The propagation of the new seed level and the response through the generator would then be computed.

## APPENDIX II. SIMPLE ELECTRICAL TRANSPORT PROPERTY FUNCTIONS FOR MHD GENERATOR PLASMAS

Electrical transport properties $\sigma$ (scalar electrical conductivity) and $\beta$ (Hall parameter) are required for the description of the flow in an MHD generator. Although quite detailed theories exist for the prediction and calculation of the electrical transport properties in MHD generator plasmas, simple functions which summarize these detailed calculations are useful for execution of the time dependent description of an MHD generator. We offer here such a set of simple electrical transport property functions.

The scalar electrical conductivity $\sigma$ and Hall parameter $\beta$ may be expressed in terms of the electron number density $n_e$ and the mobility $\mu$ as

$$\sigma = en_e\mu \tag{AII-1}$$

$$\beta = \mu B \tag{AII-2}$$

where e is the electron charge and B is the magnetic field induction. The electron number density $n_e$ may be expressed in terms of the temperature and seed density $\rho_{so}$ as

$$n_e = 1/2\ [\sqrt{K^2 + 4n_{so}K} - K] \tag{AII-3}$$

where

$$n_{so} = \rho_{so}/MW_s \tag{AII-4}$$

$$K(T) = G\left(\frac{2\pi m_e kT}{h^2}\right)\exp\ (-\varepsilon_i/kT) \tag{AII-5}$$

The seed molecular weight is $MW_s$, K(T) is the equilibrium constant expressed in terms of the statistical weight factor G, electron mass $m_e$ and Planck constant h.

The electron mobility may be expressed as

$$\mu = [\mu_o^{-1}(\frac{\rho}{\rho_r})f(\frac{T}{T_r}) + \mu_s^{-1}(\frac{n_{so}-n_e}{n_{sr}})f_s(\frac{T}{T_r}) + \mu_c^{-1}(\frac{n_e}{n_{so}})(\frac{T}{T_r})^{-3/2}]^{-1} \quad \text{(AII-6)}$$

The quantities $\mu_o$, $\mu_s$, $\mu_c$, $\rho_r$, $n_{sr}$, $T_r$ are parameters which summarize the cross section and number density dependence of the various collision terms. The first term on the right hand side of (AII-6) represents the bulk gas contribution to the mobility. The second term represents the seed contribution. The third term represents the Coulomb contribution. The functions $f_o(\frac{T}{T_r})$, $f_s(\frac{T}{T_r})$ represent the temperature dependence of the bulk gas and seed thermal speed-cross section functions. For a constant cross section species composing the bulk gas, the function $f_o$ is given by

$$f_o(\frac{T}{T_r}) = (\frac{T}{T_r})^{1/2}$$

The foregoing functions for $n_e$ and $\mu$ represent simple summary formulas for the electrical transport processes. These functions require the parameters

$MW_s$, $G$, $\varepsilon_i$ for the electron number density

and

$\mu_o$, $\mu_s$, $\mu_c$, $\rho_r$, $n_{sr}$, $T_r$, $f_o$, $f_s$ for the electron mobility

Given these parameters, the thermodynamic state variables $\rho$, $\rho_{so}$, $T$ are then required to determine $\sigma$, $\beta$.

For combustion product gases in the range 1750-3000° K and 0.1-10 atmospheres pressure seeded with potassium, suitable values for the parameters are

$\mu_o^{-1} = 0.70 \quad (m^2/\text{volt-sec})^{-1}$

$\mu_s^{-1} = 0.12 \quad (m^2/\text{volt-sec})^{-1}$

$\mu_c^{-1} = 14.5 \quad (m^2/\text{volt-sec})^{-1}$

$n_r = 3 \times 10^{24} m^{-3}$

$n_{sr} = 1.5 \times 10^{22} m^{-3}$

$T_r = 2500°\ K$

$f_o(\xi) = \xi^a \ ; \ a = 0.2$

$f_s(\xi) = \xi^b \ ; \ b = 0.2$

## REFERENCES


1. E. P. Velikhov, "Hall Instability of Current Carrying Ionized Plasmas," Proc. MHD Electrical Power Generation, New Castle Upon Tyne, 1962, p. 135-136.

2. J. E. McCune, "Wave Growth and Instability in Partially Ionized Gases," Proc. Symposium on Engr. Aspects of MHD, Paris, 1964, p. 523-538.

3. J. K. Wright, "A Temperature Instability in Magnetohydrodynamic Flow," Proceedings of the Physical Society, Vol. 81, 1963, p. 498-505.

4. P. Lax and B. Wendroff, Comm. Pure Appl. Math., Vol. 13, 1960, p. 217.

5. R. Richtmyer and H. K. Morton, Difference Methods for Initial Value Problems, 2nd Ed., J. Wiley and Son, New York, 1967.

6. R. W. MacCormack and A. J. Paulley, AIAA Paper, No. 72-154, 1972.

7. R. Courant, K. Friedricks, and H. Lewey, Math. Ann., 100, 1928, p. 32.

8. E. U. Locke and J. E. McCune, "Growth Rates for Axial Magneto Acoustic Waves in a Hall Generator," AIAA Journal, Vol. 4, 1966, p. 1748-1751.

9. W. L. Powers and J. B. Dicks, "Transient Wave Growth in Magnetogasdynamic Generators," AIAA Journal, Vol. 6, p. 1007-1012.

10. S. Jardin, "A Numerical Investigation of Unsteady Magnetogasdynamics," M.S. Thesis, Dept. of Nuclear Engr. and Dept. of Physics, Massachusetts Institute of Technology, June 1973.

11. D. A. Oliver and S. Jardin, "Nonlinear Stability of Magnetohydrodynamic Generators," to be submitted to the 1974 AIAA Fluid and Plasmadynamic Conference.

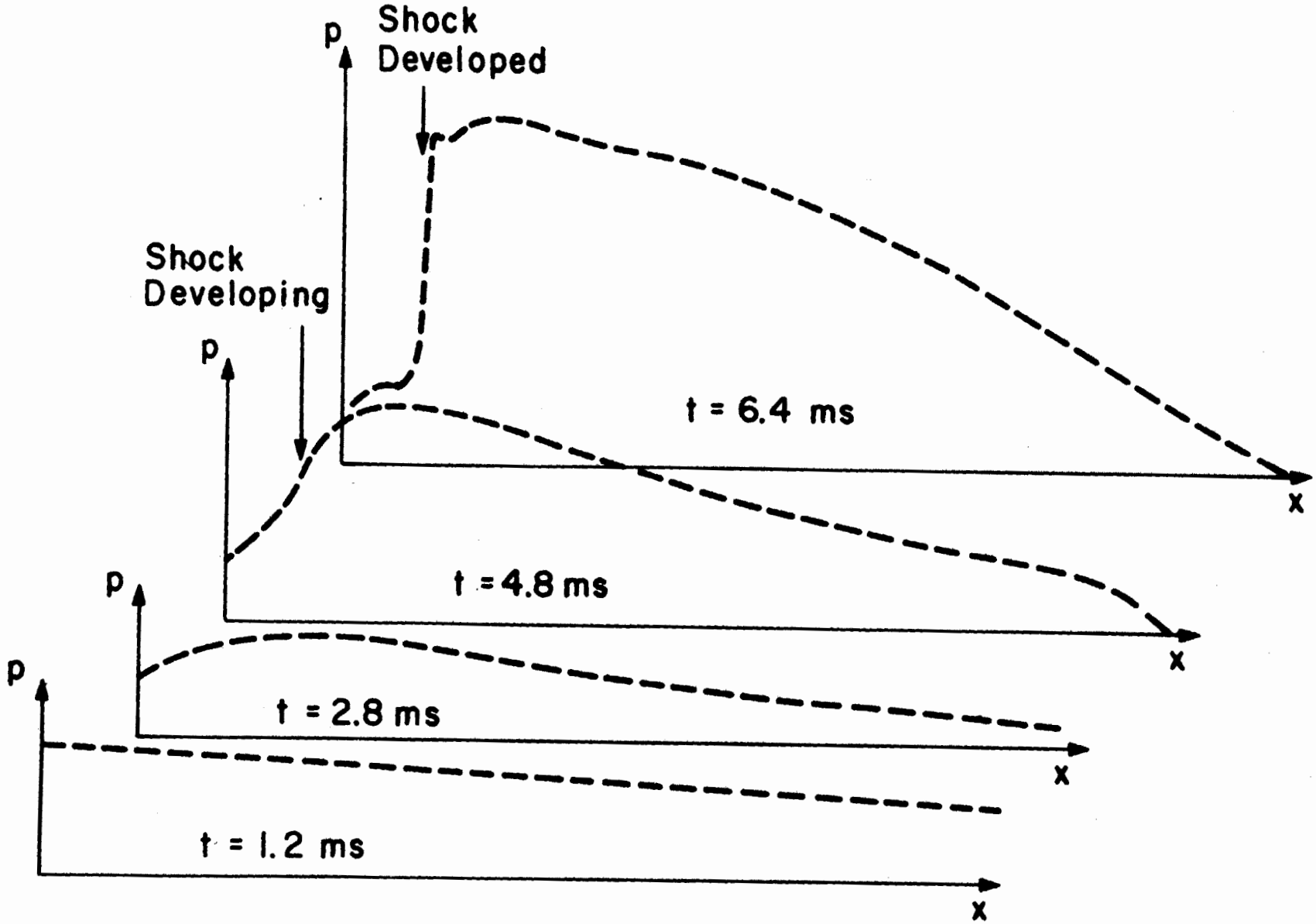


Fig. 1. Pressure distribution - time history of generator design of Table VI-1 subjected to sudden imposition of short circuit at time t = 0.

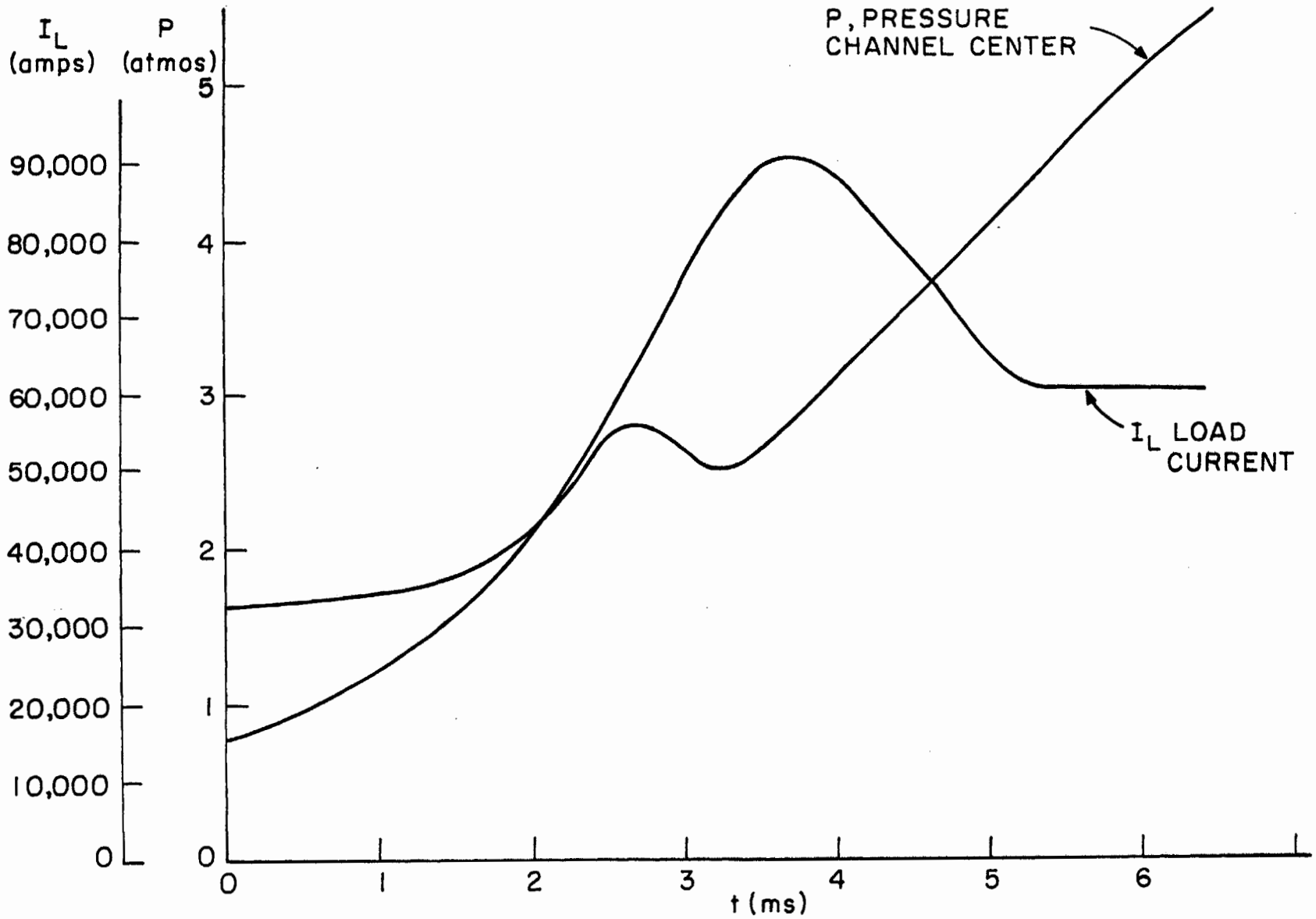


Fig. 2. Load current and channel pressure response to sudden imposition of short circuit to the generator design in Table VI-1.

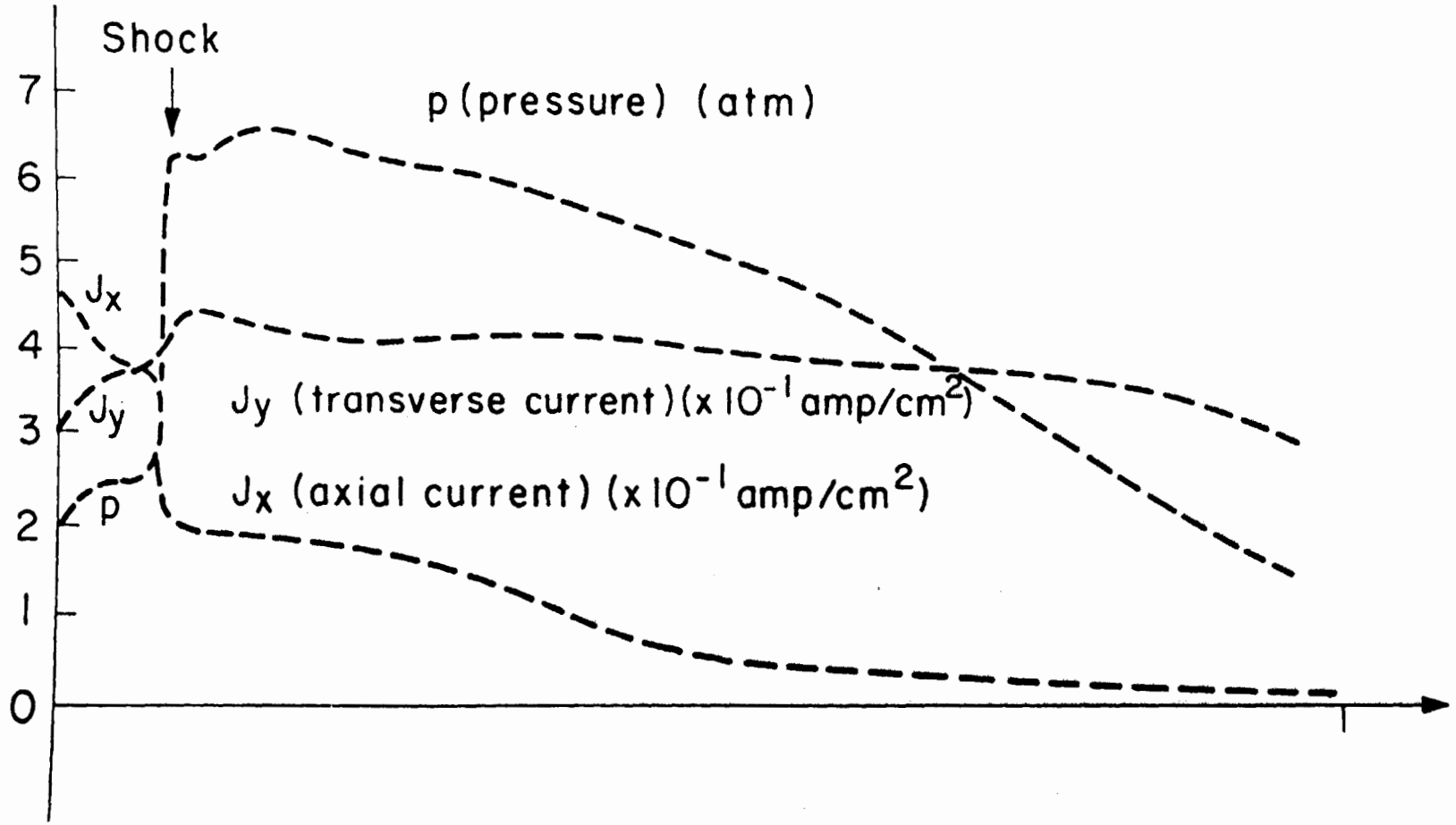


Fig. 3. Pressure and current distribution at t = 6.4 ms in the generator design of Table VI-1 subjected to load short at t = 0.

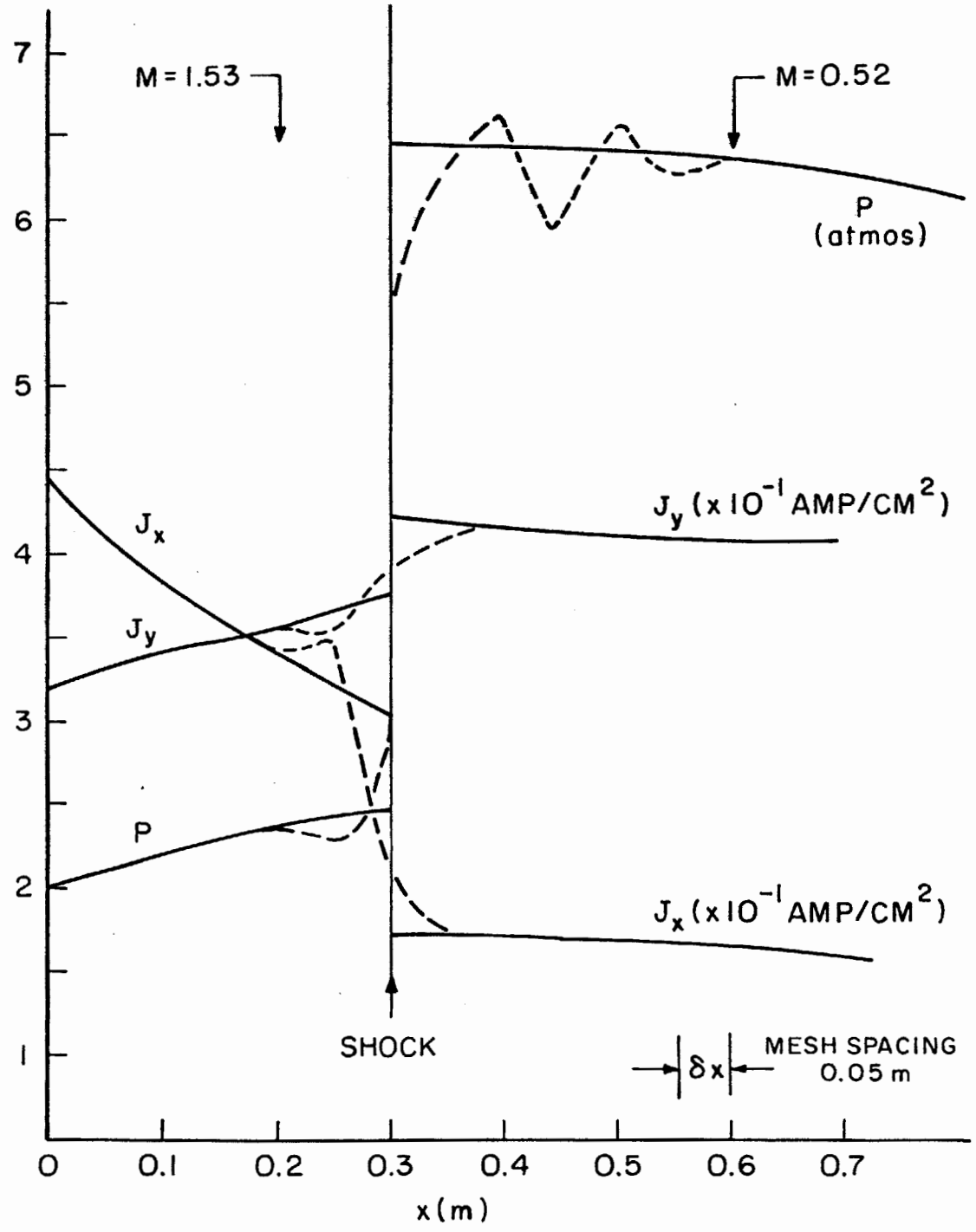


Fig. 4. Current and pressure distribution in the vicinity of the shock wave (generated by the imposition of short circuit on the generator design of Table VI-1 at t = 6.43 ms. (----- computed solution by finite difference method, ——— actual distribution)

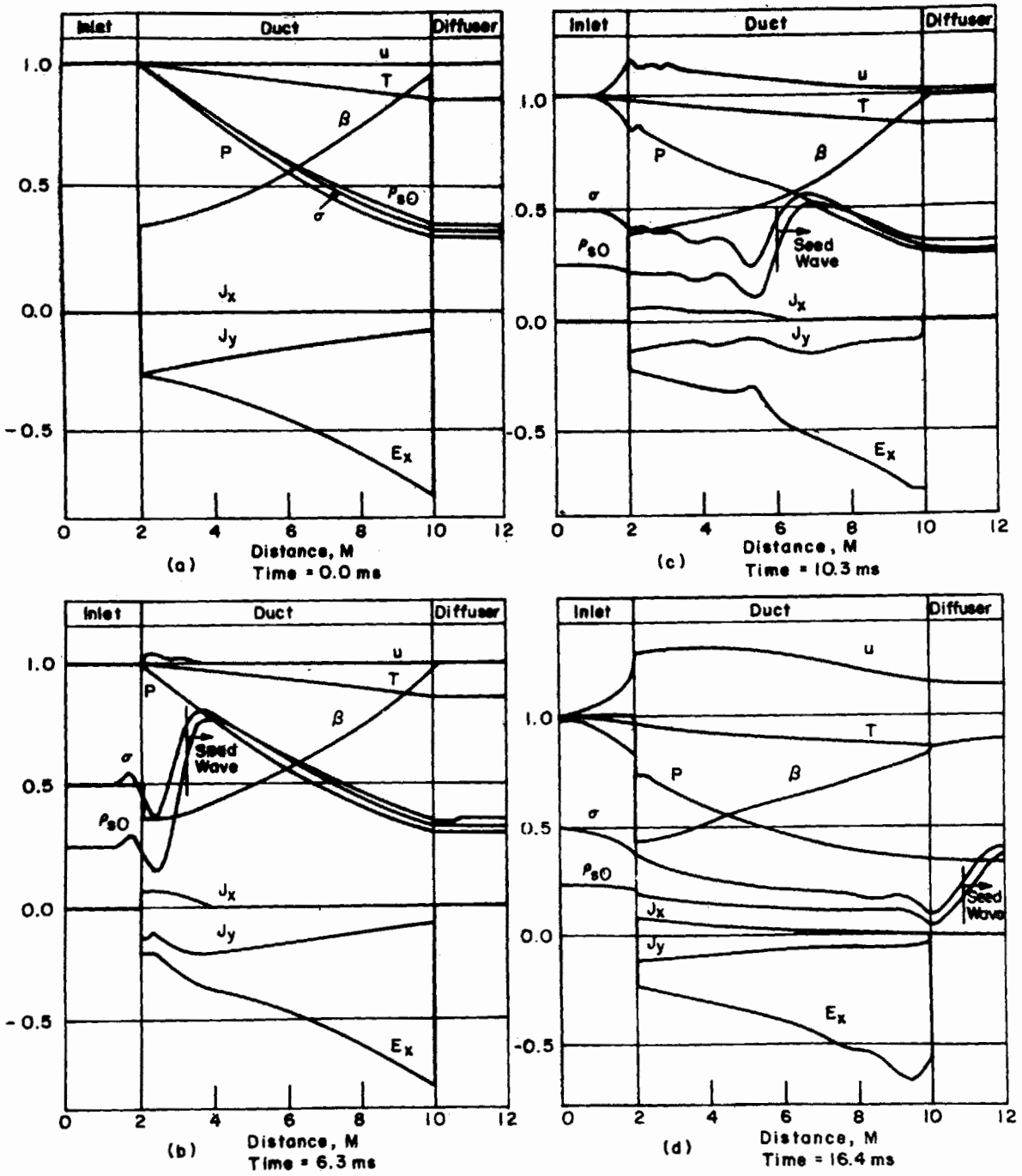


Fig. 5. Response of generator design in Table VI-2 subjected to a four-fold reduction in inlet seed density at time = 2 ms. Note advancing seed density wave, reduced transverse current $J_y$, and developing axial current $J_x$ in wake of seed density wave. Note propagation of seed density wave which has completely swept through generator by t = 16.4 ms.

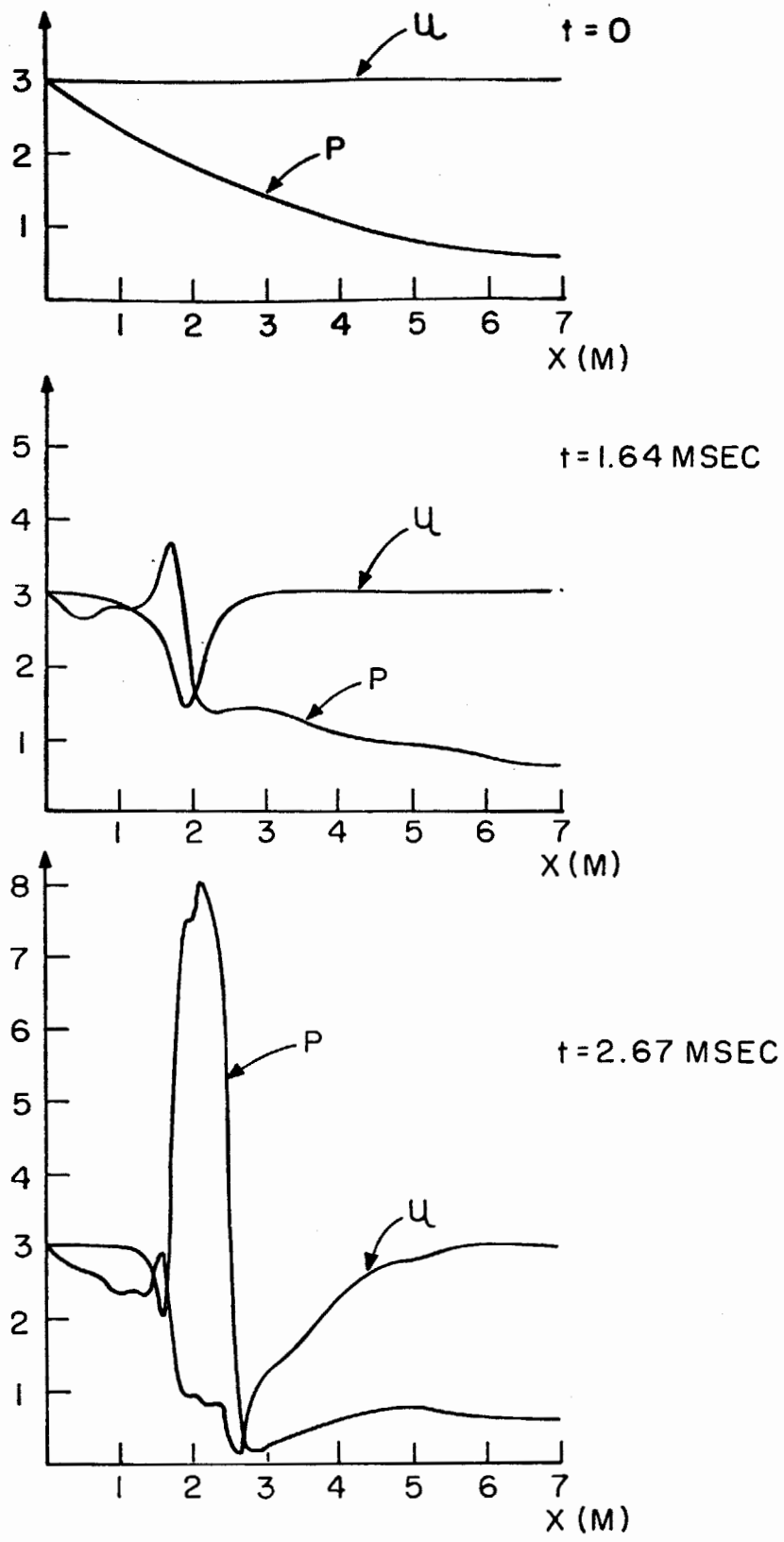


Fig. 6. Development of massive Instability from a convective instability initiated by a finite amplitude pressure pulse $\frac{\Delta p}{p_i} = 0.06$ for the generator design of Table VII-1.